



Investigative Modeling of New Pathways for Secondary Organic Aerosol Formation

Final Report
CRC Project A-59

Prepared for

Coordinating Research Council, Inc.
3650 Mansell Road
Suite 140
Alpharetta, Georgia 30022

Prepared by

Betty K. Pun and Christian Seigneur
Atmospheric and Environmental Research, Inc.
2682 Bishop Drive
Suite 120
San Ramon, California 94583

CP213-01-01

March 2006

PREFACE

This document represents the final deliverable to the Coordinating Research Council under Project A-59. It represents the state of the science as of December 2005. Because new information continues to appear in the scientific literature at a rapid pace, this document will not be submitted for publication in the peer-reviewed literature in its current form.

LEGAL NOTICE

This report was prepared by Atmospheric and Environmental Research, Inc. (AER) as an account of work sponsored by the Coordinating Research Council (CRC). Neither the CRC, members of the CRC, AER, nor any person acting on their behalf: (1) makes any warranty, express or implied, with respect to the use of any information, apparatus, method, or process disclosed in this report, or (2) assumes any liabilities with respect to the use, inability to use, or damages resulting from the use or inability to use, any information, apparatus, method, or process disclosed in this report.

Investigative Modeling of New Pathways for Secondary Organic Aerosol Formation

Betty K. Pun and Christian Seigneur

Atmospheric and Environmental Research, Inc., 2682 Bishop Drive, Suite 120, San Ramon, CA 94583

Version date: 20 March 2006

Abstract

Recent advances in secondary organic aerosol (SOA) research are reviewed and the status of current understanding is investigated with a model of SOA formation. Benzene and isoprene are newly identified precursors that are included here in the SOA model; these precursors form SOA via secondary products. The model is also extended to include some representation of aqueous partitioning and the formation of high molecular weight products via oligomerization. Experimental data and empirical relationships are used where possible; however, a detailed representation of SOA formation is not feasible given the current state of information. Sensitivity studies are conducted with the SOA model and SOA predictions are found to be very sensitive to the treatment of the interactions between particulate water and organic compounds. Influential model formulation parameters include the aerosol partitioning ratios for several small products of isoprene and the partitioning constants for unidentified products that are currently derived by fitting experimental data. The pH value used as the reference for the activation of oligomerization is also a critical parameter. Recommendations for future work needed to improve SOA models include the elucidation of the water-organic relationship, the extent of phase separation, and laboratory experiments conducted under conditions more relevant to ambient studies (e.g., lower concentrations, higher relative humidity).

Introduction

Most three-dimensional air quality models use aerosol modules that are based on the state-of-the-science from the late 1990s, including the partition of anthropogenic and biogenic secondary organic aerosols (SOA) based on empirical data from smog chambers (e.g., Odum et al., 1997; Griffin et al., 1999), with a correction factor applied to the equilibrium constant based on temperature (Strader et al., 1999; Pun et al., 2003). A few models have limited treatment of aqueous dissolution (e.g., Jacobson, 1997; Pun et al., 2002; Griffin et al., 2003). The early 2000s have seen major advances in SOA research. Precursors have been identified that were previously believed not to lead to SOA formation, including benzene (Martin-Reviejo and Wirtz, 2005) and isoprene (Jang et al., 2002; Czoschke et al., 2003; Claeys et al., 2004a, b; Matsunaga et al., 2005). New processes have been identified that may lead to significant SOA formation, including oligomerization (Jang and Kamens, 2001; Jang et al., 2002; Czoschke et al., 2003; Limbeck et al., 2003; Gao et al., 2004b; Iinuma et al., 2004; Jang et al., 2005) and cloud processes (Warneck, 2003; Ervens et al., 2004a, 2004b; Lim et al., 2005). In light of the poor model performance typical of PM models for organic aerosols (e.g., Seigneur and Moran, 2004), it is desirable to incorporate recent advances in SOA research into models to obtain an understanding of the impact of new pathways even though our theoretical understanding of many SOA forming processes is still incomplete. Such investigative modeling will allow us to identify the most uncertain parameters and processes and to recommend experiments needed to develop improved models of SOA formation.

In the current study, we focus on gas-phase, gas/particle partitioning and particulate-phase processes. Aqueous-phase reactions in clouds are not considered. An investigative SOA box model is formulated based on a synthesis of published information. Sensitivity tests are then conducted to understand the parameters and conditions that influence SOA prediction. Based on these results, recommendations are made for additional information that will be the most useful to improve the formulation of more accurate SOA models.

Benzene

The yields of SOA from benzene range from 8 to 25% based on recent chamber data from Martin-Reviejo and Wirtz (2005). They found that the formation of SOA from benzene occurs only after the consumption of a threshold amount of benzene. Both the threshold and final SOA yield depend on NO_x concentrations. The presence of NO_x delayed SOA formation but enhanced the total amount formed. They also concluded that the formation of SOA does not occur as a first oxidation step, but as a result of the oxidation of secondary compounds, including ring-retaining products and ring-opening products. Because many uncertainties still exist in the reaction mechanism of benzene degradation, a semi-empirical approach is, therefore, used here to incorporate the formation of SOA from benzene into models.

While there have been several attempts to develop detailed mechanisms for benzene degradation, condensed mechanisms are typically used in three-dimensional models of air quality. Such condensed mechanisms typically represent first reaction steps, generic secondary radicals, and lumped products. Here, we choose to start with a benzene reaction used in the Statewide Air Pollution Research Center (SAPRC) mechanism (Carter, 1990; 1996), as shown in Table 1. The three first-step oxidation products (besides peroxy radicals) are phenol, glyoxal and a lumped species representing ring-opening products. The stoichiometric coefficients of the reaction were determined based on model fits to environmental chamber data.

Phenol is an intermediate reactant that can lead to the formation of aromatic compounds with multiple substituents (e.g., nitrophenol, catechol) that may become SOA precursors. The reaction $\text{PHENOL} + \text{OH}$ may be added to a mechanism that does not track PHENOL (OH may then be added as a product to retain the original chemical dynamics) or condensable products may be added to an already existing reaction. We assume that the yield of SOA from phenol is analogous to the yield of SOA from toluene and other monosubstituted aromatic compounds based on Odum et al. (1997). Therefore, the reaction of PHENOL with OH forms the condensable compounds PHENAER1 and

PHENAER2 (see Table 1 for stoichiometric coefficients). The partitioning coefficients of PHENAER1 and PHENAER2 are 0.053 and 0.0019 m³/μg, respectively at 298 K. Because the partitioning characteristics of PHENAER1 and PHENAER2 are the same as those of TOLAER1 and TOLAER2, the condensable products may be lumped in SOA modules based on Odum et al. (1997) with suitable corrections for the differences in molecular weight (MW).

Anhydrous glyoxal is a liquid at ambient temperature. It has a vapor pressure of approximately 18 torr (0.02 atm) at 20 °C (Hastings et al, 2005), and is, therefore, not very condensable. However, in chamber experiments, glyoxal condenses at concentrations as low as 5 ppb (Liggio et al., 2005) and 0.1 torr (~100 ppm) when relative humidity (RH) is greater than 26% (Hastings et al., 2005). The partitioning into an aqueous phase is enhanced by the formation of ethan-tetrol (glyoxal monomer dihydrate) and oligomers of the hydrate molecules. The effective Henry's law constant (H_{eff}), i.e., the ratio of aqueous monomer and dihydrate concentrations to the gas-phase glyoxal concentration, is 3.6×10^5 M/atm. The equilibrium constant for the formation of dimer (concentration of dimer over the square of the concentration of hydrate) is 0.56 M^{-1} at 25 °C. Thus, in the ambient atmosphere, where glyoxal concentrations range from 0.1 to 3 ppb, the monomer dihydrate form is favored. Therefore, for the partitioning of glyoxal, a formulation that represents the effective partitioning due to the hydrated form is used (see Table 1). This formulation, therefore, requires the inputs of liquid water content (LWC) and RH as inputs.

The formation of oligomers from glyoxal and glyoxal hydrate is likely to be the rate-limiting step to aerosol growth, whereas the hydration reaction is fast. There are likely other factors that affect the rate of oligomer formation, e.g., pH, aerosol composition. Oligomerization may further modify the effective partition behavior, and is discussed below.

Koehler et al. (2004) suggested that furandione (a product of benzene oxidation with a gas-phase yield ~ 4%) can react with water to form dicarboxylic acid in the particulate

phase. Acidity can subsequently increase the partitioning of aldehydes into the particulate phase, presumably due to enhanced oligomerization in the presence of acids. These processes are not represented here because of a lack of quantitative information.

Glyoxal is also expected to participate in cloud processes (Lim et al., 2005) to give rise to oxalic acid, which can result in SOA formation if the cloud droplet evaporates to form a particle. This process needs to be incorporated in a cloud module and, therefore, is not represented here in the aerosol module.

As a group, ROP (ring-opening products) include many yet unidentified, multifunctional compounds. Some members of this group are aerosol precursors (e.g., muconaldehyde) and there is no a priori basis to define their partitioning characteristics or those of their products. To form second-generation products, ROP are expected to react with OH (Carter et al., 1996). Partitioning characteristics of ROP are determined as described next so that 8-25% of the reacted benzene forms aerosols under dry conditions (Martin-Reviejo and Wirtz, 2005).

Four condensable products are assumed to be formed in the reactions of benzene (see Table 1): two second-generation products originating from the reactions of phenol, glyoxal, and a lumped second-generation product via ring-opening reactions. In theory, a portion of the ROP products is expected to be condensable, characterized by some partitioning coefficient. Because of the uncertainties associated with the amount of ROP formed and subsequently reacted, a two-parameter characterization seems incompatible with available mechanistic data. One approach is to use a default stoichiometric coefficient of 1 for a condensable product from ROP, and to derive a partitioning coefficient for this condensable product. The partitioning coefficient is treated as an adjustable parameter to achieve the experimental yields of 8-25%. In this case, the experimental conditions of Martin-Reviejo and Wirtz (2005) were used. Glyoxal formation was considered to be negligible due to the use of low RH experimental conditions and the SOA mass was, therefore, assumed to consist of AROPA, APHENA1, and APHENA2. The yields of APHENA1 and APHENA2 were estimated for those

experiments, assuming the reactions were complete when the maximum mass of particles was formed. First, the total amount of each condensable phenol product was estimated based on the amount of reacted benzene and the stoichiometry of phenol and PHENAER species, corrected for the difference in MW. Then, the amounts of particulate phase APHENA1 and APHENA2 were estimated based on the partitioning constant and the total amount of particulate matter (PM) present in the environmental chamber. The amount of AROPA was then estimated from the difference between the experimental SOA yield and the estimated yields of APHENA1 and APHENA2. The gas-phase concentration of ROPAER was calculated from the stoichiometry of the reaction and the amount of reacted benzene. For each experiment, the partitioning coefficient of ROPAER was then calculated using the ratio of mass fraction in the particulate phase to the gas-phase concentration. The average partitioning coefficient for ROPAER was calculated to be $0.0013 \text{ m}^3/\mu\text{g}$, with a range of 0.0008 to $0.0022 \text{ m}^3/\mu\text{g}$.

Isoprene

The formation of SOA from isoprene is supported by both ambient observations as well as smog chamber and laboratory studies (Claeys et al., 2004a, b; Edney et al., 2005; Kroll et al., 2005; Limbeck et al., 2003; Matsunaga et al., 2005). Several theories are available. The first one is the gas-phase formation of condensable compounds. Kroll et al. (2005) reported 0.9 to 3.0% (by mass) yield of SOA from gas-phase reactions. Under their experimental conditions, the OH + isoprene reaction was expected to dominate over the O₃ + isoprene reaction. Oxidation reactions of isoprene products such as methacrolein, 3-methylfuran and other minor products are postulated to lead to SOA formation. With ammonium sulfate seeds, Kroll et al. found no evidence of high molecular weight products.

Edney et al. (2005) found evidence for an “SO₂”-assisted mechanism for SOA formation. Among SOA products, they found 2-methylglyceric acid and 2-methyl-butyl-1,2,3,4-tetrols, and attributed the remaining SOA mass to oligomers. Claeys et al. (2004a, b) proposed mechanisms to form 2-methylglyceric acid and 2-methyl-butyl-1,2,3,4-tetrols

from the reaction of isoprene. In their subsequent paper, they disputed the mechanism proposed in the original paper, which required gas-phase reactions under low NO_x conditions. Their current theory involves the reaction of isoprene and methacolein (a first-generation isoprene product) with H_2O_2 in acidic particles. (The authors concluded that the lifetime of the reaction is inconsistent with the lifetimes of clouds.) The proposed reaction is analogous to the oxidation of SO_2 . Previous work has concluded that SO_2 oxidation occurs mostly in cloud droplets because the same reactions in aqueous particles cannot be significant due to the very low liquid water constant volume available for reaction (Saxena and Seigneur, 1987; Meng and Seinfeld, 1994). Since isoprene is less soluble than SO_2 , the reaction in aqueous particles cannot account for the di- and tetra-hydroxy products and such reactions are more likely to occur in clouds. As mentioned above, we do not attempt here to represent cloud reactions.

The second mechanism is the formation of high MW products or oligomers in the presence of acid catalysts (Czoschke et al., 2003; Limbeck et al., 2003), which will be discussed below.

Matsunaga et al. (2005) found that in the ambient atmosphere, small multifunctional compounds, such as glycolaldehyde (GLYALD), hydroxyacetone (HYACET), and methylglyoxal (MGLY), show much higher affinity towards the particle phase than predicted based on their Henry's law constants. The observed aerosol partition ratio (APR; the dimensionless ratio of the particulate-phase concentration over the total [gas + particulate] concentration) correlates linearly with RH, and the authors proposed oligomerization as a possible reason. A process similar to the one for glyoxal, discussed above, may be one mechanism responsible for enhanced particulate-phase concentrations.

Another mechanism that has been explored involves aqueous reactions in clouds (e.g., Lim et al., 2005; Ervens et al., 2004a,b; Warneck, 2003). As mentioned above, our focus here is to investigate aerosol processes; cloud processes are discussed extensively in the publications referenced above.

The exact mechanism for SOA formation from isoprene has not been elucidated, and factors affecting each potential process, e.g., competing oxidants, NO, RH, to name a few, are still being studied. At this time, we use the following framework (Table 2) to incorporate several of the theories for enhanced partitioning, including the formation of SOA from second-generation products, enhanced solubility of small multifunctional compounds, and the oligomerization of relatively volatile species.

We start with the gas-phase reactions for isoprene from the SAPRC mechanism (Carter and Atkinson, 1996), although similar gas-phase reactions are available in many common mechanisms. The main gas-phase products, methacrolein (MACR) and methylvinylketone (MVK), are tracked specifically, but other products are lumped into unidentified isoprene products (ISOPRD). The SAPRC mechanism accounts for the fate of the isoprene products relating to O₃ production. Here, we focus only on second-generation products leading to the formation of SOA.

Matsunaga et al. (2005) expected the partitioning of GLYALD, HYACET, and MGLY to be a function of RH. Based on ambient observations, they reported a linear fit of the APR as a function of RH, but the coefficients of determination were low ($r^2 = 0.4, 0.2,$ and 0.2 for three compounds) due to significant scatter of the data. GLYALD, HYACET, and MGLY are small compounds with two hydrophilic functional groups, some of which interact with protons. At any given RH, ambient particles can be associated with different amounts of water and proton concentrations due to differences in inorganic and organic PM composition. Such differences can account for the range of partitioning characteristics. An inspection of the data reveals that the RH effect may be modeled more appropriately in terms of ranges of separate values of APR for specific ranges of RH, as shown in Table 2, rather than with a weak linear correlation between APR and RH.

Although MACR is fairly volatile, its partitioning is considered here because this compound is structurally similar to many that are considered to be active towards oligomerization.

Based on experiments described in Kroll et al. (2005), SOA yields from the isoprene + OH reaction ranged from 0.9 to 3%. The chamber results are consistent with the stoichiometric yields of Carter, and the values of the APRs towards the low end of the ambient values observed in Matsunaga et al. (2005). This indicates that the aerosol formed in the experimental chamber contained little water compared to ambient aerosols, which is consistent with the use of aqueous ammonium sulfate seed at RH of 0.4 to 0.5. No SOA is formed from MVK in the chamber and the SOA yield from MACR is 2.2%. Based on the MACR stoichiometric coefficient and MW, SOA formation from MACR accounts for about 0.5% ($2.2\% \times 0.23 \times 70/68$) of the SOA yield of the reaction of isoprene with OH. The remainder of the SOA yield, 0.4 to 2.5%, must be accounted for by products of ISOPRD, assuming first-generation products to be volatile. Therefore, since the stoichiometric coefficient of ISOPRD is 0.36, the second-generation SOA yield from ISOPRD is estimated to be between 1% and 7%.

Based on a procedure similar to that used for benzene for the estimation of the partitioning coefficient for ROPAER, the partitioning coefficient for ISPRAER was determined using the chamber data of Kroll et al. (2005) based on the model formulation in Table 2. When the SOA due to GLYALD, HYACET, and MGLY was subtracted from the experimental aerosol yield, the partitioning coefficient of a second-generation condensable product from ISOPRD was estimated to be $0.0008 \text{ m}^3/\mu\text{g}$, with a range of 0 to $0.0048 \text{ m}^3/\mu\text{g}$. We assume this partitioning coefficient also applies to the products of the unidentified product of the ozone reaction. (Henze and Seinfeld [2006], based on data from Kroll et al. [2006], proposed an absorption model involving two surrogate products to represent the formation of SOA from isoprene under low NO_x conditions.)

Oligomerization

Partitioning module formulation. The term oligomerization is used here to describe a range of processes that form high MW compounds. To date, several reactions have been postulated to contribute to the formation of high MW species in SOA, including

hemiacetal and acetal formation, trioxane formation, polymerization, aldol condensation (Jang et al., 2003, 2005), and peroxyhemiacetals (Johnson et al., 2005; Docherty et al., 2005). However, the precursors and oxidants involved, condensing species that are subject to oligomerization, and the environmental conditions favorable for such reactions remain poorly characterized. It is possible that multiple processes, including ones not yet identified, are involved in the formation of high MW compounds in the ambient atmosphere. A few studies have attempted to account for association reactions by assuming stable, nonvolatile products that increase SOA mass via irreversible reactions (e.g., Johnson et al., 2005). This assumption may be an oversimplification because (1) current laboratory data support a hypothesis that such products may decompose back to precursor species (e.g., Hastings et al., 2005; Ziemann, 2005) (hence they may not be detectable in routine experiments) and (2) some theoretical calculations show that the high MW products formed are not always thermodynamically favored over the lower MW reactants (Barsanti and Pankow, 2004, 2005). Kroll and Seinfeld (2005) show that if a partitioning compound reacts further in the particulate phase, then as long as the final product is less volatile than the partitioning species, an apparent partitioning constant can be used to describe the system to account for the abundance of SOA due to the particulate phase reaction. Such a formulation seems appropriate to represent SOA oligomerization.

One school of thought involves acid-catalyzed association or oligomerization reactions (Gao et al., 2004; Jang et al., 2005). Aldehyde moieties have been found to be more reactive than ketones (Jang et al., 2003, 2005) in acid-catalyzed association reactions. (Double bonds are also postulated to be a candidate reactant [Limbeck et al. 2003] for oligomerization.) Jang et al. (2005) derived a semi-empirical yield expression for oligomeric products based on an aldehyde hydrate undergoing polymerization, and generalized it to a variety of reactions. In that formulation (M. Jang, personal communication, 2006), the so-called “second-order relative organic aerosol yield” (Y) (proportional to a mass fraction equilibrium relationship) is defined as

$$Y = \frac{10^{-3} MW_i \cdot OM}{M_{seed} (K_p C_{init})^2} \quad (1)$$

where MW_i is the MW of the monomer compound i , OM represents the mass (mg/m^3 air) of the higher MW compounds, M_{seed} (mg/m^3 air) is the concentration of initial particulate matter (seed) in the experiment, K_p is the equilibrium partitioning coefficient of the monomer between the gas and particulate phases and C_{init} is the initial concentration of the monomer in the gas phase (mg/m^3 air). The term $K_p * C_{\text{init}}$ represents the monomer mass fraction in the particulate phase that is in equilibrium with the gas phase under experimental conditions. This yield is proportional to the second-order partitioning coefficient assuming the self reaction of i in the particulate phase:

Monomer + Monomer \leftrightarrow High MW Product (oligomer)

$$K_{eq} = \frac{[oligomer_i]}{[monomer_i]^2} \quad (2)$$

where $[x]$ represents the particulate phase concentration (mole/L) of x . To account for ambient conditions rather than experimental conditions, we calculate the “second-order relative organic aerosol yield” Y where M_{AOM} replaces M_{seed} as the absorbing medium, and $C_{g,i}$ (gas-phase concentrations) replaces C_{init} (initial concentrations). Note that for ambient concentrations, $\mu\text{g}/\text{m}^3$ is the more appropriate concentration units compared to mg/m^3 . The yield in the ambient atmosphere, Y_a , is then expressed as follows:

$$Y_a = \frac{10^{-3} MW_i \cdot OM}{M_{AOM} (K_p C_{g,i})^2} \quad (3)$$

The monomer mass fraction in the particulate phase is equal to $K_p C_{g,i}$. In the ambient atmosphere, self reactions are less likely because a mixture of condensable species is present. Therefore, we define an analogous equilibrium relationship for a monomer reacting with a pool of other monomers (assumed to be constant), such that a first order “effective” equilibrium coefficient can be defined to be proportional to Y_a .

$$K_{o,i} = \frac{[oligomer_i]}{[monomer_i] \cdot \sum_j [monomer_j]} \quad (4)$$

$$\frac{[oligomer_i]}{[monomer_i]} = K_{o,i} \sum_j [monomer_j] = K_{o,eff,i}$$

where $K_{o,i}$ is the equilibrium constant for the formation of higher MW product from monomer i , $C_{monomer,i}$ is the concentration of monomer i in the particulate phase, $\sum_j monomer_j$ is the total concentration of all monomer species that can participate in the oligomerization reaction (e.g., all compounds containing the aldehyde functional group) and $K_{o,eff,i}$ is a first-order effective equilibrium constant for the formation of higher MW products from monomer i . We assume that, since $K_{o,i}$ is proportional to Y , it has the same parametric dependence as Y in Jang et al. (2005).

Y was found to depend on several parameters, including the excess acidity (X), pH, the basicity constant of the monomer species (i.e., the equilibrium constant for the protonated form of the isomer, K_{BH^+}), and the hydration constant (i.e., the equilibrium constant for the hydrated form of the monomer). Of these parameters, the hydration constant depends on the structure of the reacting compounds and is assumed to be constant for a given class of compounds. For the compounds tested in Jang et al. (2005), aldehydes were about two orders of magnitude more reactive towards oligomerization than ketones. Therefore, as a first approximation, only aldehyde groups are assumed to participate in oligomerization reactions. The empirical model of Jang et al. (2005) is simplified to:

$$\log Y = x X + z Z + r \log (K_{BH^+}) + 11.79 \quad (5)$$

where Z is the pH function ($Z = \log(C_{H^+} a_w)$, where C_{H^+} is the proton concentration (mole/L) and a_w is the water activity (=RH)). X is a function of proton concentrations and activity coefficients of the species involved in the protonation reaction of carbonyl functional group; X was also found to be strongly correlated to RH. The hydration constant for aldehyde species is already taken into account in the intercept term. For

example, conjugation with a double bond was found to increase the stability of the protonated form. At this point, detailed molecular structure information is not available to support the model representation of SOA species beyond surrogate structures. Therefore, a constant value was assumed for K_{BH^+} for all aldehyde-containing species. Jang et al. (2005) also found that two of the parameters, X and Z, are strongly negatively correlated. Since X is supposed to increase linearly with RH ($X = 0.0372 (\%RH) - 3.716$) (Jang et al., 2003) and a_w is by definition equal to RH, the negative correlation indicates the overwhelming driving force associated with the concentration of protons. Although the presence of some water is necessary for the presence of protons, water dilutes the concentration of SOA and may slow down oligomerization when present in high concentration. There is, at present, no information on how much water is necessary to trigger oligomerization reactions. Using a theoretical approach, Pun et al. (2005) showed that SOA formed from common anthropogenic and biogenic precursors may be associated with up to $5 \mu\text{g}/\text{m}^3$ of water, depending on RH and the characteristics of SOA. A relative oligomerization yield can be defined using a simple relationship with the concentration of protons.

$$\log(Y/Y_{\text{ref}}) = z \log(C_{H^+} / C_{H^+, \text{ref}}) \quad (6)$$

where $z=1.91$ based on Jang et al. (2005). We further assume that the ratio of the effective first-order equilibrium constants (monomer + all aldehydes) is the same as the ratio of the second-order equilibrium constants. Therefore, for species i ,

$$\log\left(\frac{K_{o,i}}{K_{o,i,\text{ref}}}\right) = \log\left(\frac{Y_i}{Y_{i,\text{ref}}}\right) = z \log\left(\frac{C_{H^+}}{C_{H^+,\text{ref}}}\right) \quad (7)$$

If we assume that the equilibrium aldehyde monomer concentration does not change with pH (i.e., only the concentration of the protonated monomer does), then the ratio of $K_{o,\text{eff},i}$ will be the same as the ratio of $K_{o,i}$.

$$\log\left(\frac{K_{o,eff,i}}{K_{o,eff,i,ref}}\right) = \log\left(\frac{K_{o,i} \cdot \sum_j [monomer_j]}{K_{o,i,ref} \cdot \sum_j [monomer_j]_{ref}}\right) = \log\left(\frac{K_{o,i}}{K_{o,i,ref}}\right) \quad (8)$$

The definition of $K_{o,eff,i,ref}$ and $C_{H^+,ref}$ is problematic, because the experiments carried out to date have typically been designed to maximize the formation of oligomers via the use of acidic seeds, high concentrations of reactants, or the addition of co-reactants that enhance the formation of oligomers. Gao et al. (2004) used several experimental conditions involving acidic and non-acidic seed particles. They estimated the mass fraction of oligomers to be at least 10%, with the lower end value associated with a concentration of H^+ due to the intrinsic production of organic acids from the reaction system producing SOA. Therefore, we use a reference value of 0.1 for $K_{o,eff,ref}$ at a moderate pH of 6.

A module for simulating SOA needs to be computationally efficient if it is to be used for three-dimensional applications. Accordingly, most SOA models employ a surrogate representation or a hybrid one with surrogates and explicit species. For organic precursors, hundreds of SOA products can be formed and a surrogate representation is almost necessary for a majority of the products. As a starting point, the aerosol yield data from Odum et al. (1997) and Griffin et al. (1999) are used (e.g., Zhang et al., 2004). In that formulation, each precursor compound is associated with one or two surrogate products. The SOA yield of each surrogate product depends on two parameters, one representing the mass-based stoichiometric coefficient (α) and one representing a partitioning coefficient (K_p). K_p is corrected for temperature using the Clausius-Clapeyron equation assuming an enthalpy of vaporization of 72.7 kJ/mol. Because oligomerization is typically catalyzed by protons, interaction with water is implicitly assumed. The inclusion of water in the absorbing medium necessitates another correction of K_p based on the MW (Pankow, 1994). In the dry chamber experiments, the empirical K_p reflects the absorption into an SOA phase. With water interaction, the MW of the absorbing medium will typically decrease, hence increasing the value of K_p .

Smog chamber experiments described in Odum et al. (1997) and Griffin et al. (1999) were conducted in relatively dry conditions that are not conducive to oligomerization. We assume that the experimental K_p values represent a situation where the condensed mixture contains mostly monomers, with a minimal amount (10%) of oligomers. When polymerization takes place, α does not change, but the effective K_p increases. From Kroll and Seinfeld (2005):

$$K_{p,\text{eff}} = K_p(1+K_{o,\text{eff}}) \quad (8)$$

At experimental conditions, we assume $K_{p,i,\text{eff}} = C_i / (M * C_{g,i})$, where C_i is the particulate-phase concentration of species i , M is the mass of all absorbing compounds, and $C_{g,i}$ is the gas-phase concentration of i , all of which are in $\mu\text{g}/\text{m}^3$ air.

$$K_{p,\text{eff}} = C_{\text{monomer},i} / (M * C_{g,i}) + C_{\text{highMWspecies},i} / (M * C_{g,i}) \quad (9)$$

where $C_{\text{highMWspecies},i}$ is the concentration of higher MW species. At the reference conditions of the “dry” experiments: $C_{\text{highMWspecies},i} = 0.1 C_{\text{monomer},i}$. Therefore, $K_{p,\text{eff}} = 1.1 C_{\text{monomer},i} / M / C_{g,i} = 1.1 K_p$. Therefore,

$$K_{o,\text{ref},i} = C_{\text{highMWspecies},i} / (M * C_{g,i}) \big|_{\text{at reference conditions}} = 0.1 K_p$$

Under conditions that promote the formation of oligomers, $K_{o,\text{eff}}$ will change with pH and thus, $K_{p,\text{eff}}$ will change.

Oligomer-forming species. Among the SOA mixture, we assume that species containing aldehyde groups are the main candidates for oligomer reactions. Therefore, for each surrogate condensing species, the fraction of compounds containing aldehyde groups, hence subject to oligomerization, is determined. Identified SOA and condensable products for all precursor species were compiled from the literature, including experimental and modeling studies (see Literature Review document, Pun and Seigneur, 2005, Yu et al., 1999; Glasius et al., 2000; Larsen et al., 2001; Jaoui and Kamens, 2001,

2003; Griffin et al., 2002). The condensable products were grouped into species that contain aldehyde groups (subject to oligomerization) and monomer species that contain no aldehyde groups. Based on the total (gas and particle yields) of each identified condensable product documented in the literature, a fraction of the condensable surrogate species (Odum et al., 1997 and Griffin et al., 1999), those containing the aldehyde functionality, was determined to be subject to oligomerization for each precursor species (see Table 3).

When oligomerization is activated, the K_p value for the aldehyde fraction would increase, whereas the K_p value for the fraction not subject to oligomerization would remain the same. The net effect of oligomerization is to increase the partitioning of relatively volatile SOA into the particulate phase. Table 3 lists the precursors and reactions forming SOA species. The list of precursor species was selected based on available partitioning data from environmental chambers (Odum et al., 1997 and Griffin et al., 1999) and pruned based on similarity in chemical structure and reaction characteristics and the abundance of biogenic emissions of specific terpene compounds (Pun et al., 2004). MWs of actual SOA were used to convert the mass-based α (Odum et al., 1997 and Griffin et al., 1999) to mole-based stoichiometric coefficients. Species subject to oligomerization are notated with an AERO suffix instead of an AER suffix. Table 4 lists the subsequent equilibria of surrogate SOA species that lead to additional SOA formation via partitioning of first oxidation products toward more soluble or less volatile compounds.

Sensitivity Tests

The sensitivity tests are designed to understand the effects of changes in environmental variables on SOA formation as well as to elucidate the effects of uncertainties in model formulation and parameters on the model predictions. Test cases focus on the new precursors and processes (see Table 5), although conclusions regarding environmental conditions can be generalized to other condensing species with similar characteristics.

We consider three SOA precursors in these sensitivity tests: benzene, isoprene and α -pinene.

Benzene. According to our model, four products of benzene oxidation are available for partitioning. Their total concentrations are listed in Table 5 for the reaction of 10 ppb of benzene. The sensitivity to environmental conditions is tested first; we investigate the yields of particulate-phase organic compounds as a function of LWC, pH, and primary organic compound (POC) concentration. Second, we investigate the sensitivity of SOA yields to some model parameters.

Figure 1 shows the yield of SOA as a function of LWC, pH, and POC. The top panel of Figure 1 shows that the SOA yield is very sensitive to the LWC, with a very low yield of 2.5% when particles are quite dry to 43% when the LWC is $100 \mu\text{g}/\text{m}^3$ at pH of 4. The enhancement of SOA yield is due to several effects. First, when LWC increases, the absorbing mass (M) increases for species partitioning by Raoult's law and the solvent mass increases for compounds partitioning according to Henry's law. For the Raoult's law species, since $C_i/C_{g,i} = K_p \cdot M$, more of the available condensable compound mass enters the particulate phase. For species partitioning according to Henry's law, the dependence is also straightforward, since $C_i/C_{g,i} = H \cdot LWC$. Second, because the reference K_p values from Odum et al. (1997) and Griffin et al. (1999) were measured at dry conditions, they were corrected for the average MW for wet conditions based on Pankow (1994). Water lowers the MW of an organic mixture, thereby increasing the K_p values. Third, oligomerization can take place in an aqueous medium, further increasing the K_p values based on Equation 8.

A comparison of the results from pH = 4 and pH = 6 illustrates several effects of water on the partitioning properties of SOA. At pH = 6, oligomerization is assumed to be at a minimum value of 10%. The SOA yield at low LWC is similar at pH = 6 (2.4%) and pH = 4 (2.5%) because there is not sufficient monomer mass in the particulate phase available for oligomerization. At $100 \mu\text{g}/\text{m}^3$ LWC, the enhancement of SOA production

is smaller at pH = 6, 38% compared to 43% at pH 4. The case with pH = 6 represents the effects of water on the partition of monomers. At LWC = 1 $\mu\text{g}/\text{m}^3$, the composition of benzene SOA is 27% AROPA, 62% APHENA1, and 11% APHENA2. The partitioning at low LWC can be explained in terms of the partitioning coefficients and the total concentrations of the species, with PHENAER1 having the highest K_p and the largest ratio of C_i/C_g , followed by PHENAER2 and ROPAER. With an aerosol containing 0.76 $\mu\text{g}/\text{m}^3$ SOA, 5 $\mu\text{g}/\text{m}^3$ POC, and 1 $\mu\text{g}/\text{m}^3$ LWC, the average MW was 84. Therefore, the K_p values (which are 0.16, 0.0057 and 0.0013 $\text{m}^3/\mu\text{g}$ for pure organic aerosols) are 0.37, 0.01, and 0.0009 $\text{m}^3/\mu\text{g}$, respectively, for PHENAER1, PHENAER2, and ROPAER after correcting for MW of the absorbing medium. Despite the low K_p value of ROPAER, AROPA accounts for a larger percentage of the SOA than APHENA2 due to its total (gas + particulate) concentration, which is higher by a factor of 30 (see Table 5).

In comparison, when LWC = 100 $\mu\text{g}/\text{m}^3$ the composition of the benzene SOA is 86% AROPA, 5% APHENA1, and 9% APHENA2. At high LWC, a large percentage of the available condensables enters the particulate phase for all three partitioning compounds; therefore, the relative abundance is related to the total amount available for partitioning. With a particle that is mostly water, the average MW is 21.3. Therefore, K_p values corrected for MW are much larger than in the LWC = 1 $\mu\text{g}/\text{m}^3$ case (1.6, 0.04, and 0.004 $\text{m}^3/\mu\text{g}$, respectively, for PHENAER1, PHENAER2, and ROPAER). The mass of the particulate phase is 117 $\mu\text{g}/\text{m}^3$ (including an SOA concentration of 12 $\mu\text{g}/\text{m}^3$).

The partitioning of glyoxal is not significant when pH = 6, even though the partitioning of glyoxal increased by 2 orders of magnitude (to 0.004 $\mu\text{g}/\text{m}^3$, or 0.1% of the total available glyoxal) when LWC increases from 1 to 100 $\mu\text{g}/\text{m}^3$. This is because the Henry's law constant is 3.6×10^5 M/atm, which converts to 9×10^{-6} $\text{m}^3/\mu\text{g}$. Even at 100 $\mu\text{g}/\text{m}^3$ LWC, particle concentrations are low because $C_i/C_{i,g} = 9 \times 10^{-4}$. However, at pH = 4, the partition is enhanced due to the formation of high MW products from glyoxal. As shown in the middle panel of Figure 1, at a constant LWC content of 50 $\mu\text{g}/\text{m}^3$, SOA yields increase from 0.24 to 0.39 with decreasing pH, because particulate phase glyoxal

increases from $0.002 \mu\text{g}/\text{m}^3$ at $\text{pH} = 6$ or above (no oligomerization) to $4.8 \mu\text{g}/\text{m}^3$ at $\text{pH} = 3$. The sensitivity of the SOA predictions to the formulation of the oligomerization module is discussed further under the α -pinene case.

Because of the overwhelming proportion of water, changing the POC concentration has a limited effect on the partition of SOA. The bottom panel of Figure 1 shows cases with relatively low amount of LWC (1 and $10 \mu\text{g}/\text{m}^3$). Varying POC from 1 to $20 \mu\text{g}/\text{m}^3$ increases the SOA yield in both cases. The effect is much more pronounced when $\text{LWC} = 1 \mu\text{g}/\text{m}^3$. The SOA yield changes from 0.021 to 0.032 due to increased partitioning of PHENAER1, PHENAER2 and ROPAER. When $\text{LWC} = 10 \mu\text{g}/\text{m}^3$, increasing POC mass from 1 to $20 \mu\text{g}/\text{m}^3$ leads to a corresponding change in SOA yield from 0.079 to 0.085 . At lower LWC, POC constitutes a larger fraction of the absorbing medium and increasing POC increases the total mass available by a greater percentage than when water constitutes more of the absorbing medium.

Due to incomplete information regarding the reaction of benzene, a parameterization is used to model SOA formation processes. We investigate now the effect on SOA yields of the parametric uncertainties of the partitioning constant K_p of ROPAER and of the stoichiometric coefficient for ROP. Uncertainties in K_p were determined based on the range of K_p values ($0.0008 - 0.0022 \text{ m}^3/\mu\text{g}$) deduced from different smog chamber experiments reported by Martin-Reviejo and Wirtz (2005). In a previous version of SAPRC (Carter, 1990), the stoichiometric coefficient was 0.49 instead of 1.44 . Therefore, for the stoichiometric coefficient, we used this change as an uncertainty range for the lower-bound estimate and tested a full range of values from 0.49 to 2.39 centering around 1.44 . The results are shown in Figure 2.

The top panel shows that at moderate LWC of $50 \mu\text{g}/\text{m}^3$, the total aerosol yield increases linearly with K_p , because the particle-phase concentration of ARPOA increases linearly with K_p . The partitioning of AROPA is linear with K_p in this K_p range because there is sufficient material in the gas phase. If the K_p values were high, further increasing the K_p value would result in an asymptotic increase of AROPA yield, limited by the total mass

available. Uncertainties in the K_p value may cause the overall yield value to be uncertain by 40%. The absolute uncertainty depends on the mass of SOA formed. In the $50 \mu\text{g}/\text{m}^3$ LWC case, SOA changes by $2.2 \mu\text{g}/\text{m}^3$ (out of $7.7 \mu\text{g}/\text{m}^3$); the same uncertainty in K_p changes SOA by only $1 \mu\text{g}/\text{m}^3$ (out of $2.6 \mu\text{g}/\text{m}^3$) when $\text{LWC} = 10 \mu\text{g}/\text{m}^3$ (not shown). Most of the mass change corresponds to a change in the AROPA mass, although small changes in APHENA1 and APHENA2 occur. Changes in APHENA1 and APHENA2 would be more pronounced if AROPA constituted a larger fraction of the absorbing medium.

The bottom panel of Figure 2 shows the effects of changes in the stoichiometric coefficient of ROP, which affects the total condensable mass available for SOA formation. The relatively large uncertainty range (factor of about five) causes the SOA yield to cover a total range of about a factor of three (base case yield is 0.24), corresponding to about $4.2 \mu\text{g}/\text{m}^3$ SOA for a stoichiometric coefficient of 2.39.

Isoprene. Five condensable products (MACR, MGLY, HYACET, GLYALD and ISPRAER) are included in the model formulation. The partitioning of MACR is negligible even under conditions conducive to aqueous partition and/or oligomerization. For example, with $\text{LWC} = 100 \mu\text{g}/\text{m}^3$ and $\text{pH} = 3$ (i.e., conditions previously found to generate significant levels of glyoxal SOA), only 0.1% of the MACR mass is calculated to enter the particulate phase due to a Henry's law constant that is five orders of magnitude smaller than that of glyoxal. Therefore, MACR is not considered in the following test cases. Of the remaining products, HYACET, GLYALD, and MGLY partition based on ambient APR and ISOPRD partitions based on Raoult's law. Uncertainties in APR and the formulation of the absorption module are investigated.

The data of Matsunaga et al. (2005) that relate APR and RH show significant scatter. Therefore, we define a range of uncertainty for the APR of each species and for each RH range ($< 60\%$; $>60\%$) using the 10th and 90th percentile of the raw APR data (Matsunaga, private communication, 2006). At RH above 60%, the ranges of APR are 0.13 to 0.58, 0.11 to 0.60, and 0.17 to 0.56, respectively, for HYACET, GLYALD, and MGLY. At

RH below 60%, the ranges of APR are 0.12 to 0.36, 0.06 to 0.23, and 0.06 to 0.37, respectively, for HYACET, GLYALD, and MGLY. Results of the partition simulations using the lower and upper limit of those ranges are shown in Figure 3. Total aerosol formed can increase from the base case by 48% to 57% when higher APR values are used, depending on the RH regime. Therefore, parametric uncertainties in APR values can cause the aerosol yield to be uncertain, with ranges of 0.08-0.17 (nominal 0.12) at low RH and 0.10-0.29 (nominal 0.19) at RH above 60%.

As discussed under the formulation of the isoprene module, K_p for the unknown isoprene products leading to SOA formation was determined based on smog chamber data by making the assumption that the LWC content of the laboratory aerosols was low. An upper limit of $0.0048 \text{ m}^3/\mu\text{g}$ was calculated based on the range of deduced K_p values. When this high value of K_p was used, the yield of aerosol in the test case increases from 0.12 to 0.25, indicating the model's sensitivity to this value, due to the abundant formation of the ISOPRD product (see Figure 4).

We attempted to investigate model formulation uncertainties by comparing two other possible formulations of the Raoult's law module: (1) one in which water does not interact with organics (external mixture of organic liquid and aqueous phases) and (2) a fixed yield of SOA from the ISOPRD product. When water is excluded from the organic absorbing medium, SOA yields drop significantly because AISPRA concentrations decrease from 1.33 to $0.01 \mu\text{g}/\text{m}^3$, indicating (as suggested in the benzene test case) the sensitivity of the Raoult's law module to the mass and average MW of the absorbing medium. Even when a larger K_p value is used, only limited enhancement was found. Therefore, the role of water within a partitioning system can have significant effects on the aerosol yields in the ambient atmosphere.

Finally, a fixed yield approach was tested. The yield of AISPRA from ISOPRD was deduced to be 1-7% (Kroll et al., 2005). An average of 3.5% was used as a fixed yield in one simulation. The fixed yield approach produces an aerosol yield of 0.08 vs. the base

case yield of 0.12 and the amount of AISPRA formed is between the partition cases with or without water.

α -pinene. The partition of α -pinene products (see total concentrations in Table 5) is shown in Figure 5 as a function of pH. The amount of SOA formed is insensitive to pH when pH is above 6 because we use this pH value as our reference below which oligomerization is activated. The oligomerization correction term to the partitioning constant increases with decreasing pH, resulting in more of the product subject to oligomerization (APINAERO2) entering the particulate phase. As shown in Figure 4, the effects of oligomerization are most pronounced at a specific pH range between 5 and 6 for this case study. At pH below 4, virtually all available APINAERO2 mass resides in the particulate phase and reducing pH further results in no further increase in the SOA mass and yield. Around pH = 6, when oligomerization is activated, the mass of oligomers increases by $6 \mu\text{g}/\text{m}^3$, while the total SOA mass increases only by $2.5 \mu\text{g}/\text{m}^3$. This is because some of the material ($3.9 \mu\text{g}/\text{m}^3$) undergoing oligomerization is present in the particle as monomers at higher pH. At pH = 5, APINAERO2 is already mostly present in the particulate phase as oligomers; with the effective partitioning constant increasing nine times over the monomer value.

The fraction of each SOA that is considered to be subject to oligomerization involved assuming that aldehyde is the key functional group involved. This assumption is tested by increasing that fraction to include all carbonyl species (fraction = 1), thereby increasing the amount of oligomerizable compounds. The results are represented using open symbols in Figure 5. At high pH, when only monomers are involved in the partitioning process, the fraction of oligomerizable material is irrelevant. Increasing the oligomerizable fraction increases the potential amount of SOA and potential yield of SOA at low pH. By increasing the fraction of oligomerizable material from 0.77 to 1.0 for APINAERO2, the mass concentration of AAPINA2 increases from 8.1 to $9.1 \mu\text{g}/\text{m}^3$ (100% of the condensable material) at pH = 3. The overall SOA yield increases accordingly from 0.33 to 0.37.

Parameters used in the formulation of the SOA module are tested to understand where key uncertainties lie. Parameters are changed in the direction that leads to less oligomerization. We tested the sensitivity to $K_{o,eff,ref}$, z , and the reference pH. For $K_{o,eff,ref}$ and z , the only differences these parameters make in the partitioning of the oligomer species are simulated when the effect of oligomerization is largest (pH = 5-6). At pH = 5, lowering $K_{o,eff,ref}$ from 0.1 to 0.05 lowers the enhancement factor applied to K_p due to oligomerization from about 9 to about 5. However, the effect on the formation of SOA is small because the equilibrium is strongly displaced toward oligomers as the pH decreases by only one unit. Similarly, lowering z from 1.91 to 1.5 would result in an enhancement factor of 4 to the monomer value of K_p . The maximum effects on oligomer concentrations is only a decrease of $0.6 \mu\text{g}/\text{m}^3$ (see Figure 6).

A more important parameter seems to be the proton concentration needed to catalyze oligomerization reactions. If we assume that a lower pH (5 instead of 6) is needed before oligomerization can take place, the yield curve for oligomers is essentially shifted down one pH unit. Therefore, the reference pH value below which oligomerization becomes significant appears to be a critical parameter for an SOA model.

For this test case, once oligomerization is activated, SOA yields are not very sensitive to the parameters used in the oligomerization formulation. There is a small range of pH where the aerosol yield is sensitive to parameters used in oligomerization; at lower pH, nearly 100% of the mass enters the particulate phase. For more volatile species, the uncertainty in the formulation may be more important.

Conclusions and Recommendations

The partitioning of many organic compounds is extremely sensitive to LWC because water is an abundant absorbing medium in the ambient atmosphere. Water also facilitates the partition because it has a lower MW than most partitioning compounds, effectively diluting the particle phase concentrations on a molar basis. Known oligomerization reactions take place in an organic phase that contains water and protons. However, the

sensitivity to water may be overestimated if not all liquid water present in aerosols is available to interact with organic compounds. Our sensitivity study with the isoprene product shows that models including and excluding water from the partition calculation of organic species can give very different results. Furthermore, other physical processes can also affect the interaction between water and organic compounds, including phase separation (Erdakos and Pankow, 2004) or the formation of micelles (Tabazadeh, 2005) or inverted micelles (Cai and Griffin, 2003). Physical (phase) and chemical (activity coefficients) interactions between water and organics need to be further investigated to support accurate modeling, especially if multiple liquid phases are present in the ambient atmosphere. Laboratory experiments conducted at higher RH will help elucidate the role of water in partitioning. For example, SOA yield of 8-25% were reported based on dry chamber experiments (Martin-Reviejo and Wirtz, 2005). However, when water is considered as part of the organic-containing aerosol, SOA yield in the modeled atmosphere can be significantly larger. Such behavior remains to be verified. At present, measurement methods employed in the routine monitoring networks exclude the majority of the particulate water due to sample heating, further limiting the ability to analyze aqueous-organic interactions.

Due to incomplete information, uncertainties in SOA yields due to the formulation of the model and the selection of model parameters can be significant. The uncertainties in the predicted yield due to parameterization can be as much as those due to variabilities in the most influential ambient conditions. Therefore, further experimental work is needed to characterize the gas-phase and particulate-phase products of potentially significant SOA precursors such as benzene and isoprene. Such molecular identification work is underway for isoprene SOA (Seinfeld, J.H., private communication, February, 2006). The dependence of SOA formation on co-pollutants, such as NO_x and SO_2 , should also be accounted for to the extent possible. Quantitative yield information will be quite necessary for the development of models that can be used with more confidence.

Processes that can enhance the partition of aerosols by decreasing the volatility of end products need to be investigated further. Our sensitivity study shows that the effects of

oligomerization can increase SOA formation by orders of magnitude at low pH. However, many parameters are uncertain, and laboratory studies tend to be conducted under conditions that favor these processes. More experiments that use conditions relevant to the ambient atmosphere would provide valuable data to evaluate the importance of such processes. When such data become available, further theoretical development can be accomplished to support the development of more robust models.

Acknowledgments

The Coordinating Research Council provided funding for this work under Project A-59. The authors wish to thank the Coordinating Research Council (CRC) Atmospheric Impacts Committee for its support and constructive comments. Dr. John Seinfeld, Caltech, provided two preprints on SOA formation from isoprene. Special thanks are due to Professor M. Jang (University of North Carolina) and Dr. S. Matsunaga (National Center for Atmospheric Research) for detailed discussions of their work.

References

- Barsanti, K.C.; J.F. Pankow, 2004. Thermodynamics of the formation of atmospheric organic particulate matter by accretion reactions Part 1: aldehydes and ketones, *Atmos. Environ.*, **38**, 4371-4382.
- Barsanti, K.C.; J.F. Pankow, 2005. Thermodynamics of the formation of atmospheric organic particulate matter by accretion reactions Part 2: dialdehydes, methylglyoxal and diketones, *Atmos. Environ.*, **39**, 6597-6607.
- Cai, X., R.J. Griffin, 2003. Modeling the formation of secondary organic aerosol in coastal areas: role of the sea-salt aerosol organic layer, *J. Geophys. Res.*, **108**: D15, doi: 10.1029/2002JD003053.
- Carter, W.P.L., 1990. A detailed mechanism for the gas-phase atmospheric reactions of organic compounds, *Atmos. Environ.*, **24A**, 481-518.
- Carter, W.P.L. and R. Atkinson, 1996. Development and evaluation of a detailed mechanism for the atmospheric reactions of isoprene and NO_x, *Int. J. Chem. Kinet.*, **28**, 497-530.
- Claeys, M.; B. Graham, G. Vas, W. Wang, R. Vermeylen, et al, 2004a. Formation of secondary organic aerosols through photooxidation of isoprene, *Science*, **303**, 1173-1176.
- Claeys, M.; W. Wang, A.C. Ion, I. Kourtchev, A. Gelencsér, W. Maenhaut, 2004b. Formation of secondary organic aerosols from isoprene and its gas-phase oxidation products through reaction with hydrogen peroxide, *Atmos. Environ.*, **38**, 4093-4098.
- Czoschke, N.M.; M. Jang, R.M. Kamens, 2003. Effect of acidic seed on biogenic secondary organic aerosol growth, *Atmos. Environ.*, **37**, 4287-4299

Docherty, K.S.; W. Wu, Y.B. Lim, P.J. Ziemann, 2005. Contributions of organic peroxides to secondary aerosol formed from reactions of monoterpenes with O₃, *Environ. Sci. Technol.*, **39**, 4049-4059.

Edney, E.O.; T.E. Kleindienst, M. Jaoui, M. Lewandowski, J.H. Offenberg, W. Wang, M. Claeys, 2005. Formation of 2-methyl tetrols and 2-methylglyceric acid in a secondary organic aerosol from laboratory irradiated isoprene/NO_x/SO₂/air mixtures and their detection in ambient PM_{2.5} samples collected in the eastern United States, *Atmos. Environ.*, **39**, 5281-5289.

Erdakos, G.B., J. F. Pankow, 2004. Gas/particle partitioning of neutral and ionizing compounds to single- and multi-phase aerosol particles. 2. Phase separation in liquid particulate matter containing both polar and low-polarity organic compounds, *Atmos. Environ.*, **38**, 1005–1013.

Ervens, B.; G. Feingold, G.J. Frost, S.M. Kreidenweis, 2004a. A modeling study of aqueous production of dicarboxylic acid: chemical pathways and speciated organic mass production, *J. Geophys. Res.*, **105**, D15, doi: 10.1029/ 2003JD 004387.

Ervens, B.; G. Feingold, S.L. Clegg, S.M. Kreidenweis, 2004b. A modeling study of aqueous production of dicarboxylic acid: 2 Implications for cloud microphysics, *J. Geophys. Res.* **105**, D15, doi: 10.1029/ 2004JD 004575.

Gao, S.; M. Keywood, N. Ng, J. Surratt, V. Varutbangkul, et al., 2004 Low-molecular weight and oligomeric components in secondary organic aerosols from the ozonolysis of cycloalkenes and α -pinene, *J. Phys. Chem.*, **108**, 10147-10164

Glasius, M.; M. Lahaniati, A. Calogirou, D.D. Bella, D. Kotzias, et al., 2000. Carboxylic acids in secondary aerosols from oxidation of cyclic monoterpenes by ozone, *Environ. Sci. Technol.*, **34**, 1001-1010.

Griffin, R.J.; D.R. Cocker III, R.C. Flagan and J.H. Seinfeld, 1999. Organic aerosol formation from the oxidation of biogenic hydrocarbons, *J. Geophys. Res.*, **104**, 3555-3567.

Griffin, R., D. Dabdub, J.H. Seinfeld, 2002. Secondary organic aerosol. I. Atmospheric Chemical Mechanism for production of molecular constituents. *J. Geophys. Res.*, **107**, doi:10.1029/2001JD00541.

Griffin, R.J.; K. Nguyen, D. Dabdub and J.H. Seinfeld, 2003. A coupled hydrophobic-hydrophilic model for predicting secondary organic aerosol formation, *J. Atmos. Chem.*, **44**, 171-190.

Hastings, W.P.; C.A. Koehler, E.L. Bailey, D.O. De Hann, 2005. Secondary organic aerosol formation by glyoxal hydration and oligomer formation: humidity effects and equilibrium shifts during analysis, *Environ. Sci. Technol.*, **39**, 8728-8735.

Henze, D.K.; J.H. Seinfeld, 2006. Global secondary organic aerosol from isoprene oxidation, *Geophys. Res. Lett.*, in press.

Iinuma, Y.; O. Böge, T. Gnauk, H. Herrmann, 2004. Aerosol chamber study of α -pinene/O₃ reaction: influence of particle acidity on aerosol yields and products, *Atmos. Environ.*, **38**, 761-773.

Jacobson, M.Z., 1997. Development and application of a new air pollution modeling system, Part II: aerosol module structure and design, *Atmos. Environ.*, **31**, 131-144.

Jang, M.; R.M. Kamens, 2001. Atmospheric secondary aerosol formation by heterogeneous reactions of aldehydes in the presence of a sulfuric acid catalyst, *Environ. Sci. Technol.*, **35**, 4758-4766.

- Jang, M.; N.M. Czoschke, S. Lee, R.M. Kamens, 2002. Heterogeneous atmospheric aerosol production by acid-catalyzed particle-phase reactions, *Science*, **298**, 814 – 817.
- Jang, M., S. Lee and R.M. Kamens, 2003. Organic aerosol growth by acid catalyzed heterogeneous reactions of octanal in a flow reactor. *Atmos. Environ.*, **37**, 2125-2138.
- Jang, M.; N.M. Czoschke, A.L. Northcross. 2005a. Semiempirical model for organic aerosol growth by acid catalyzed heterogeneous reactions of organic carbonyls, *Environ. Sci. Technol.*, **39**, 164-174.
- Jaoui, M.; R.M. Kamens, 2001. Mass balance of gaseous and particulate products analysis from α -pinene + NO_x in the presence of natural sunlight, *J. Geophys. Res.*, **106**, 12541-12559.
- Jaoui, M.; R.M. Kamens, 2003a. Gas and particulate products distribution from the photooxidation of α -humulene in the presence of NO_x, natural atmospheric air and sunlight, *J. Atmos. Chem.*, **46**, 29-54.
- Johnson, D.; M.E. Jenkin, K. Wirtz, M. Martin-Reviejo, 2005. Simulating the formation of secondary organic aerosol from the photooxidation of aromatic hydrocarbons. *Environ. Chem.*, **2**, 35-48.
- Koehler, C.A; J.D. Fillo, K.A. Ries, J. T. Sanchez, D.O. DeHann, 2004. Formation of secondary organic aerosol by reactive condensation of furandiones, aldehydes, and water vapor onto inorganic aerosol seed particles. *Environ. Sci. Technol.*, **38**, 5064-5072.
- Kroll, J.H.; N.L. Ng, S.M. Murphy, R.C. Flagan, J.H. Seinfeld, 2005. Secondary organic aerosol formation from isoprene photooxidation under high-NO_x conditions, *Geophys. Res. Lett.*, **32**, L18808, doi:10.1029/2005GL023637.

- Kroll, J.H.; J.H. Seinfeld, 2005. Representation of secondary organic aerosol laboratory chamber data for the interpretation of mechanisms of particle growth, *Environ. Sci. Technol.*, **39**, 4159-4165.
- Kroll, J.H.; N.L. Ng, S.M. Murphy, R.C. Flagan, J.H. Seinfeld, 2006. Secondary organic aerosol formation from isoprene photooxidation, *Environ. Sci. Technol.*, in press.
- Larsen, B.R.; D. D. Bella, M. Glasius, R. Winterhalter, N.R. Jensen, J. Hjorth, 2001. Gas-phase OH oxidation of monoterpenes: gaseous and particulate products, *J. Atmos. Chem.*, **38**, 231 – 276.
- Liggio, J.; S.M. Li, R. McLaren, 2005. Heterogeneous Reactions of glyoxal on particulate matter: identification of acetals and sulfate esters, *Environ. Sci. Technol.*, **39**, 1532 – 1541.
- Lim, H.-J.; A.C. Carlton, B.J. Turpin, 2005. Isoprene forms secondary organic aerosol through cloud processing: model simulations, *Environ. Sci. Technol.*, **39**, 4441-4446.
- Limbeck, A; M. Kulmala, H. Puxbaum, 2003. Secondary organic aerosol formation via heterogeneous reaction of gaseous isoprene on acidic particles, *Geophys. Res. Lett.*, **30** doi: 10.1029/ 2003GL017738.
- Matsunaga, S.N.; C. Wiedinmyer, A.B. Guenther, J.J. Oriando, T.Karl, D.W. Toohey, J.P. Greenberg, Y. Kajii, 2005. Isoprene oxidation products are a significant atmospheric aerosol component, *Atmos. Chem. Phys. Discuss.*, **5**, 11143-11156.
- Martin-Reviejo, M.; K. Wirtz, 2005. Is benzene a precursor for secondary organic aerosol? *Environ. Sci. Technol.* ,**39**, 1045-1054.
- Meng, Z. and J.H. Seinfeld, 1994. On the source of the submicron droplet mode of urban and regional aerosols, *Aerosol Sci. Technol.*, **20**, 253-265.

Odum, J.R., T.P.W. Jungkamp, R.J. Griffin, H.J.L. Forstner, R.C. Flagan, J.H. Seinfeld, 1997. Aromatics, reformulated gasoline, and atmospheric organic aerosol formation. *Environ. Sci. Technol.*, **31**, 1890-1897.

Pankow, J.F., 1994. An absorption model of the gas/aerosol partitioning involved in the formation of secondary organic aerosol. *Atmos. Environ.*, **28**, 189-193.

Pun, B.K.; R.J. Griffin, C. Seigneur, J.H. Seinfeld, 2002. Secondary organic aerosol: II. comprehensive thermodynamic module for gas/particle partitioning of molecular constituents, *J. Geophys. Res.*, **107 (D17)**, doi: 2001D000542.

Pun, B.K.; S.-Y. Wu; C. Seigneur; J.H. Seinfeld; R.J. Griffin; S. N. Pandis, 2003. Uncertainties in modeling secondary organic aerosols: Three-dimensional modeling studies in Nashville/Western Tennessee. *Environ. Sci. Technol.*, **37**, 3647-3661

Pun, B.K., C. Seigneur and E. Knipping, 2004, Optimizing secondary organic aerosol representation in particulate matter air quality models, Air & Waste Management Association Visibility Specialty Conference – Regional and Global Perspectives on Haze: Causes, Consequences and Controversies, 26-29 October 2004, Asheville, North Carolina.

Pun, B. K. and C. Seigneur, 2005. Secondary organic aerosols: A literature review. Project A-59, Coordinating Research Council, Alpharetta, GA.

Pun, B.K.; C. Seigneur, J. Pankow, E. Chang, R. Griffin, E. Knipping, 2005. An upgraded absorptive secondary organic aerosol partitioning module for three-dimensional air quality applications, American Association of Aerosol Research Conference, October 2005, Austin, TX,

Saxena, P. and C. Seigneur, 1987. On the oxidation of SO₂ to sulfate in atmospheric aerosols, *Atmos. Environ.*, **21**, 807-812.

Seigneur, C. and M. Moran., 2004. Chapter 8: Chemical transport models, in *Particulate Matter Science for Policy Makers: A NARSTO Assessment*, pp. 283-323, P.H. McMurry, M. Shepherd and J. Vickery, eds., Cambridge University Press, Cambridge, United Kingdom.

Strader, R., F. Lurmann, S.N. Pandis, 1999. Evaluation of secondary organic aerosol formation in winter, *Atmos. Environ.*, **39**, 4849-4864.

Tabazadeh, A., 2005. Organic aggregate formation in aerosols and its impact on the physicochemical properties of atmospheric particles. *Atmos. Environ.*, **39**, 5472-5480

Warneck, P., 2003. In-cloud chemistry opens pathway to the formation of oxalic acid in the marine atmosphere, *Atmos. Environ.*, **37**, 2423-2427.

Yu, J., R.C. Flagan and J.H. Seinfeld, 1998. Identification of products containing –COOH, –OH and –C=O in atmospheric oxidation of hydrocarbons, *Environ. Sci. Technol.*, **32**, 2357-2370.

Zhang, Y., B. Pun, K. Vijayaraghavan, S.-Y. Wu, C. Seigneur, S. Pandis, M. Jacobson, A. Nenes and J.H. Seinfeld, 2004. Development and application of the Model of Aerosol Dynamics, Reaction, Ionization and Dissolution, *J. Geophys. Res.*, **109**, D01202, doi:10.1029/2003JD003501.

Ziemann, P.J., 2005. Aerosol products, mechanisms, and kinetics of heterogeneous reactions of ozone with oleic acid in pure and mixed particles, *Faraday Discuss.*, **130**, 469-490.

Table 1. SOA-forming process for benzene

Type ⁽¹⁾	Reaction or equilibrium	Rate constant ⁽²⁾ or equilibrium constant ⁽³⁾
G	BENZENE + OH → 0.24 PHENOL + 0.21 GLYOXAL + 1.44 ROP + 0.24 HO2 + 0.76 RO2 ⁽⁴⁾	$2.5 \times 10^{-12} \exp(-0.397 / RT)$ cm ³ /molecule/s
G	PHENOL + OH → 0.071 PHENAER1 + 0.138 PHENAER2 + OH ⁽⁵⁾	2.63×10^{-11}
K	PHENAER1 ↔ APHENA1	0.053 ⁽⁶⁾
K	PHENAER2 ↔ APHENA2	0.0019 ⁽⁶⁾
H	GLYOXAL ↔ AGLYO ⁽⁷⁾	0 if RH < 26% 3.6×10^5 if RH ≥ 26% ⁽⁸⁾
G	ROP + OH → ROPAER	1.14×10^{-11}
K	ROPAER ↔ AROPA	0.0013 ⁽⁹⁾

(1) Type is either G, K, or H. G is used for gas-phase reactions, K is used for gas/particle equilibrium reactions, H is used for gas/particle equilibrium reactions where the particulate phase is aqueous. (2) Reaction rate constants are given in cm³/molecule/s. If the Arrhenius form is used, R is 0.0019872 kcal/deg K/mole. (3) Gas/particle equilibrium constants (K) are given in m³/μg. Henry's law constants (or effective Henry's law constants) are given in M/atm. (4) ROP stands for ring-opening products. RO2 represents a generic peroxy radical that reacts with NO to give NO₂. (5) The experimental mass-based stoichiometric factors are used as the molar stoichiometric coefficients, implicitly assuming that the PHENOL, PHENAER1, and PHENAER2 share the same molecular weight. The molar yield can be adjusted if the MW of the condensable products are assumed to be different from the MW of PHENOL. (6) At 310 K. (7) AGLYO stands for the aqueous forms of glyoxal including the glyoxal monomer hydrate (ethan-tetrol). (8) Effective H due to hydration; H_{eff} can be adjusted to account for oligomerization (e.g., as a function of pH). (9) Determined based on experimental data and SOA model formulation, see text.

Table 2. SOA-forming process for isoprene

Type ⁽¹⁾	Reaction or equilibrium	Rate constant ⁽²⁾ , equilibrium constant ⁽³⁾ or aerosol partitioning ratio ⁽⁴⁾
G	ISOPRENE + OH → 0.91 RO2 + 0.09 RNO3 + 0.62 HCHO + 0.23 MACR + 0.32 MVK + 0.36 ISOPRD ⁽⁵⁾	$2.5 \times 10^{-11} \exp(408 / T)$
G	ISOPRENE + O3 → 0.27 OH + 0.066 RO2 + 0.008 RNO3 + 0.59 HCHO + 0.1 ISOPRD + 0.39 MACR + 0.16 MVK + 0.2 HCOOH + 0.15 RCOOH ⁽⁵⁾	$7.86 \times 10^{-15} \exp(-1912 / T)$
G	ISOPRENE + NO3 → 0.19 NO2 + 0.75 RO2 + 0.064 RNO3 + 0.94 ISOPRD ⁽⁵⁾	$3.03 \times 10^{-12} \exp(-448 / T)$
G	ISOPRD + OH → ISPRAER	6.19×10^{-11}
K	ISPRAER ↔ AISPRA	0.0008 ⁽⁶⁾
G	MVK + OH → 0.7 GLYALD + 0.3 MGLY ⁽⁵⁾	$4.14 \times 10^{-12} \exp(453 / T)$
G	MACR + OH → 0.42 HYACET + 0.08 MGLY ⁽⁵⁾	$1.86 \times 10^{-11} \exp(176/T)$
H	MGLY ↔ AMGLY	0.21 if RH < 60% 0.25 if RH ≥ 60% ⁽⁴⁾
H	HYACET ↔ AHYACET	0.24 if RH < 60% 0.36 if RH ≥ 60% ⁽⁴⁾
H	GLYALD ↔ AGLYALD	0.10 if RH < 60% 0.36 if RH ≥ 60% ⁽⁴⁾
H	MACR ↔ AMACR	6.5 ⁽⁷⁾

(1)-(3) see notes for Table 1. (4) aerosol partitioning ratio (P/(G+P) – observation based, representing effective partitioning (including effects of oligomerization); values represent the median observed value at each RH range (raw APR data from Matsunaga, private communication, 2006); (5) RNO3 stands for alkyl nitrates; HCHO is formaldehyde; MACR is methacrolein; MVK is methyl vinyl ketone; ISOPRD is other isoprene products; HCOOH is formic acid; RCOOH is acetic acid; GLYALD is glycolaldehyde; HYACET is hydroxyacetone; MGLY is methylglyoxal; (6) Determined based on experimental data and SOA model formulation, see text. (7) Henry's law constant for MACR may be modified based on oligomerization (see below).

Table 3. Aerosol-forming reactions for surrogate precursor compounds (only SOA products are listed).

Precursor compound (molecular weight)	Gas-Phase Reactions	Rate constants (cm ³ molec ⁻¹ s ⁻¹) ⁽¹⁾
Toluene and other high SOA yield aromatics (92)	TOL + OH → 0.118 GLYOXAL + 0.131 MGLY + 0.033 TOLAER1 + 0.830 TOLAER2 ^(2,3)	1.81 x 10 ⁻¹² exp (-0.397/RT)
Xylene and other low SOA yield aromatics (106)	XYL + OH → 0.108 GLYOXAL + 0.370 MGLY + 0.023 XYLAER1 + 0.046 XYLAER2 + 0.070 XYLAERO2 ^(2,3)	1.73 x 10 ⁻¹² exp (0.705/RT)
Humulene (206)	HUM + OH → 0.847 HUMAERO	2.93 x 10 ⁻¹⁰
Limonene (136)	LIM + OH → 0.168 LIMAER1 + 0.039 LIMAER2 + 0.251 LIMAERO2	1.71 x 10 ⁻¹⁰
α-pinene (136)	APIN + OH → 0.028 APINAER1 + 0.061 APINAER2 + 0.199 APINAERO2	5.37 x 10 ⁻¹¹
	APIN + O ₃ → 0.089 APINAER3 + 0.033 APINAER4 + 0.046 APINAERO4	8.66 x 10 ⁻¹⁷
β-pinene (136)	BPIN + OH → 0.092 BPINAER1 + 0.038 BPINAER2	7.89 x 10 ⁻¹¹
	BPIN + O ₃ → 0.019 BPINAER3 + 0.423 BPINAER4 + 0.032 BPINAERO4	1.36 x 10 ⁻¹⁷
	BPIN + NO ₃ → 0.739 BPINAER5	2.31 x 10 ⁻¹²
Terpinene (136)	TER + OH → 0.058 TERAER1 + 0.397 TERAERO2	2.7 x 10 ⁻¹⁰
Terpinenol (154)	TPO + OH → 0.035 TPOAER1 + 0.052 TPOAERO2	1.59 x 10 ⁻¹⁰

(1) R is 0.0019872 kcal/deg K/mol; k from Carter (1990) for toluene and xylene and from Pun et al., 2003 and references therein for biogenic compounds. (2) yields of GLYOXAL and MGLY are from Carter, 1990. (3) although cresol, a gas-phase product can probably lead to the formation of SOA, in a manner analogous to phenol (see Table 1), cresol products are probably already accounted for in TOLAER1 and TOLAER2.

Table 4. Aerosol-forming equilibria for SOA compounds produced precursors.

SOA (molecular weight)	Equilibrium Type ⁽¹⁾	Equilibrium	Equilibrium constant @ 298K
GLYOXAL (58)	H	GLYOXAL ↔ AGLYO	see Table 1
MGLY (72)	H	MGLY ↔ AMGLY	see Table 2
TOLAER1 (198)	K	TOLAER1 ↔ ATOLA1	0.16
TOLAER2 (153)	K	TOLAER2 ↔ ATOLA2	0.0057
XYLAER1 (175)	K	XYLAER1 ↔ AXYLA1	0.13
XYLAER2 (152)	K	XYLAER2 ↔ AXYLA2	0.0042
XYLAERO2 (152)	K	XYLAERO2 ↔ AXYLAO2	0.0042 or f(pH)
HUMAERO (243)	K	HUMAERO ↔ AHUMAO	0.15 or f(pH)
LIMAER1 (198)	K	LIMAER1 ↔ ALIMA1	0.16
LIMAER2 (171)	K	LIMAER2 ↔ ALIMA2	0.016
LIMAERO2 (171)	K	LIMAERO2 ↔ ALIMAO2	0.016 or f(pH)
APINAER1 (186)	K	APINAER1 ↔ AAPINA1	0.51
APINAER2 (171)	K	APINAER2 ↔ AAPINA2	0.012
APINAERO2 (171)	K	APINAERO2 ↔ AAPINAO2	0.012 or f(pH)
APINAER3 (191)	K	APINAER3 ↔ AAPINA3	0.26
APINAER4 (174)	K	APINAER4 ↔ AAPINA4	0.24
APINAERO4 (174)	K	APINAERO4 ↔ AAPINAO4	0.24 or f(pH)
BPINAER1 (192)	K	BPINAER1 ↔ ABPINA1	0.13
BPINAER2 (147)	K	BPINAER2 ↔ ABPINA2	0.015
BPINAER3 (193)	K	BPINAER3 ↔ ABPINA3	0.58
BPINAER4 (152)	K	BPINAER4 ↔ ABPINA4	0.0090
BPINAERO4 (152)	K	BPINAERO4 ↔ ABPINAO4	0.0090 or f(pH)
BPINAER5 (184)	K	BPINAER5 ↔ ABPINA5	0.049
TPOAER1 (215)	K	TPOAER1 ↔ ATPOA1	0.48
TPOAERO2 (168)	K	TPOAER2 ↔ ATPOA2	0.013 or f(pH)
TERAER1 (217)	K	TERAERO1 ↔ ATERA1	0.24
TERAERO2 (186)	K	TERAERO2 ↔ ATERAO2	0.014 or f(pH)

(1) H: Henry's law equilibrium between the gas phase and an aqueous phase; K: aerosol-phase equilibrium

Table 5. Test cases. Nominal environmental conditions are: T = 298 K; RH = 0.5, POC = 5 $\mu\text{g}/\text{m}^3$

Case	Benzene	Isoprene	α -pinene
LWC	50 $\mu\text{g}/\text{m}^3$	50 $\mu\text{g}/\text{m}^3$	10 $\mu\text{g}/\text{m}^3$
Amount of precursor reacted	10 ppb (31.9 $\mu\text{g}/\text{m}^3$)	10 ppb (27.8 $\mu\text{g}/\text{m}^3$)	5 ppb (27.8 $\mu\text{g}/\text{m}^3$)
Condensable product = amount ($\mu\text{g}/\text{m}^3$)	glyoxal = 4.98 ROPAER = 34.2 PHENAER1 = 0.66 PHENAER2 = 1.23	ISOPRD = 10.01 HYACET = 2.92 GLYALD = 5.50 MGLY = 3.37	APINAER1 = 1.07 APINAER2 = 2.13 APINAERO2 = 6.96
Sensitivities investigated	<ul style="list-style-type: none"> ▪ LWC ▪ pH ▪ POC ▪ K_p (ROPAER) ▪ stoichiometric coefficient of ROP 	<ul style="list-style-type: none"> ▪ RH ▪ APR ▪ K_p (ISPRAER) ▪ alternative Raoult's law formulation that excludes water ▪ alternative fixed yield formulation for AISPRA 	<ul style="list-style-type: none"> ▪ pH ▪ fraction of SOA subject to oligomerization ▪ $K_{o,eff,ref}$ ▪ pH at which $K_{o,eff,ref}$ applies ▪ z

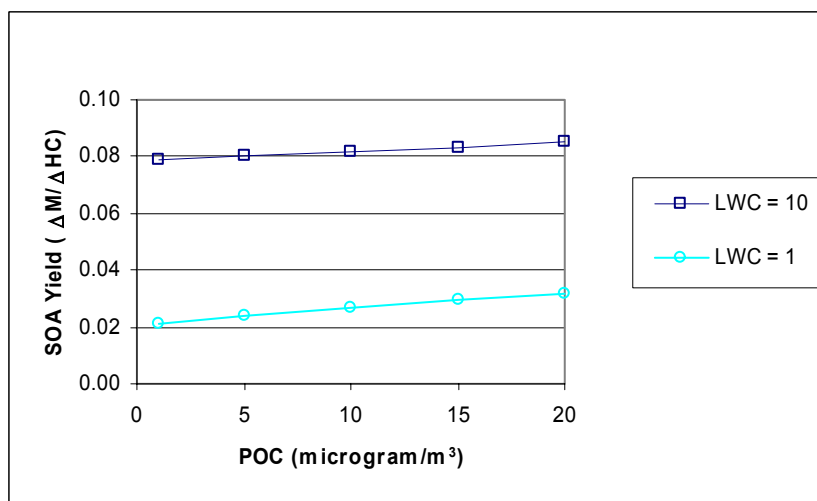
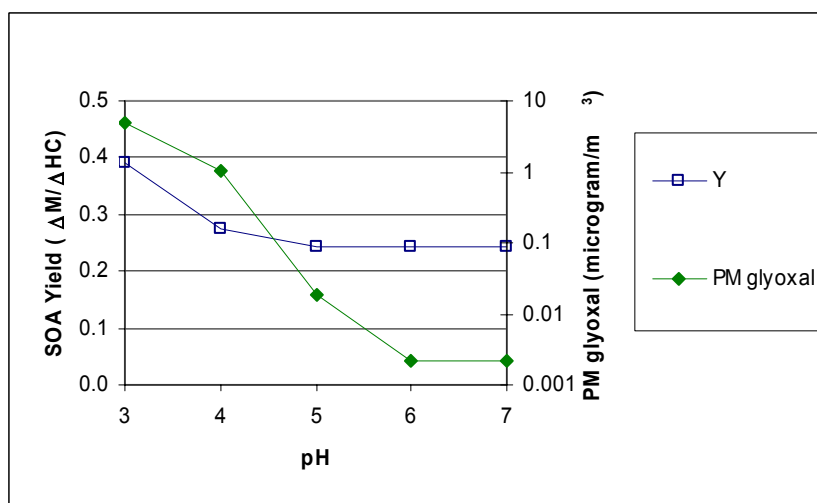
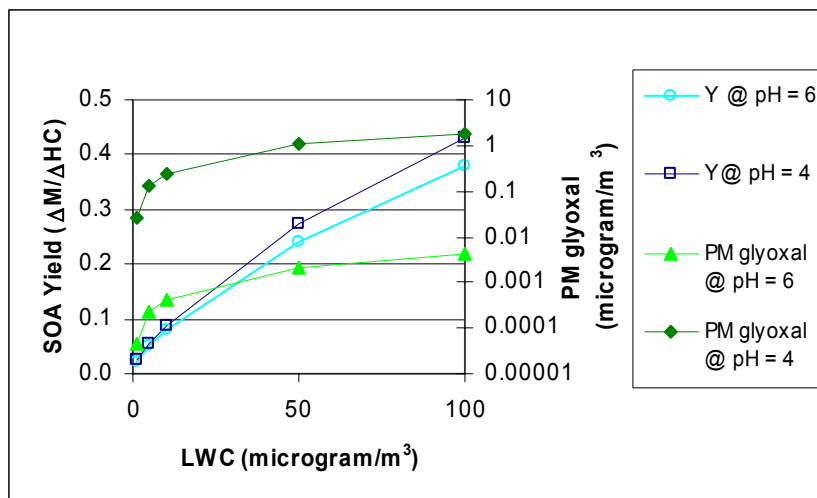


Figure 1. Benzene SOA yield as a function of LWC at pH = 4 and 6 and POC = 5 $\mu\text{g}/\text{m}^3$ (top), as a function of pH at LWC = 50 $\mu\text{g}/\text{m}^3$ and POC = 5 $\mu\text{g}/\text{m}^3$ (middle), and as a function of POC at LWC = 1 and 10 $\mu\text{g}/\text{m}^3$, pH = 6 (bottom).

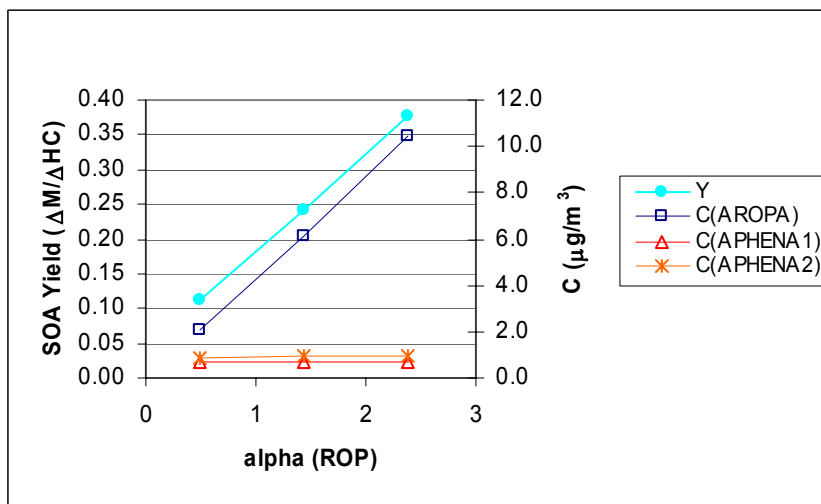
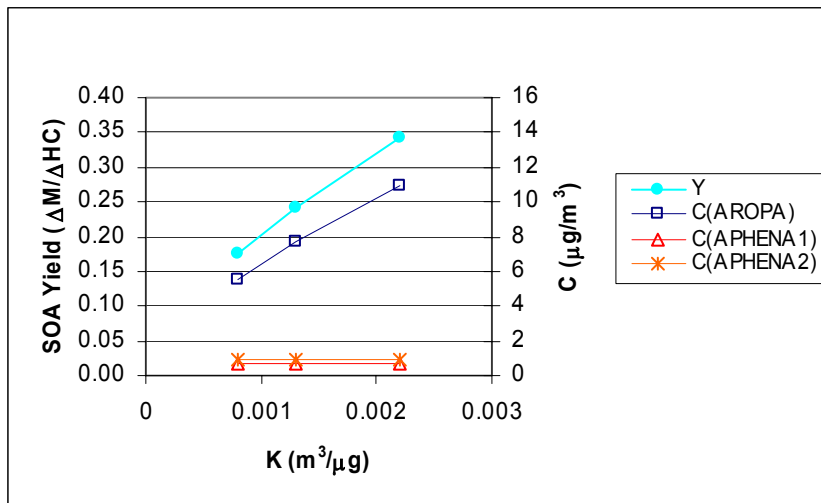


Figure 2. Benzene SOA yield as a function of K_p of the benzene ring opening product (top) and as a function of the stoichiometric coefficient of the benzene ring opening product (bottom) at $LWC = 50 \mu g/m^3$ and $pH = 6$.

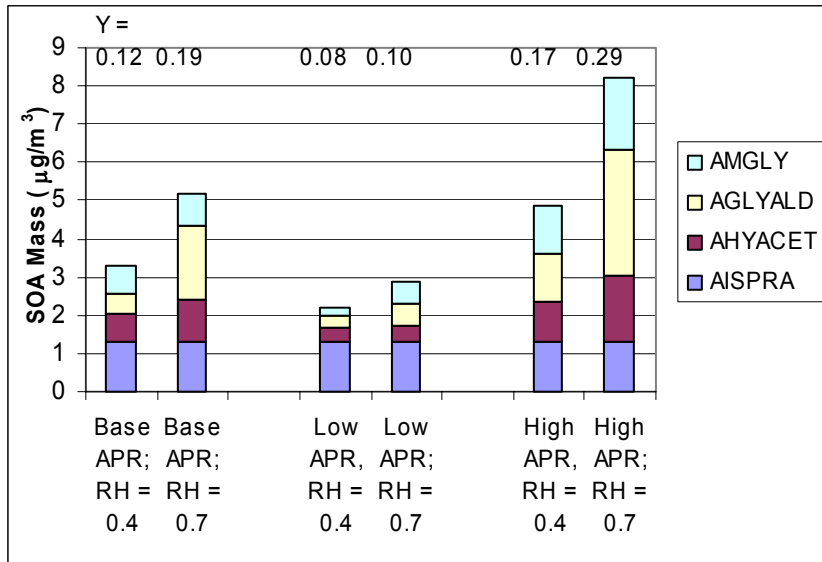


Figure 3. Mass and yield of isoprene SOA as a function of RH and APR

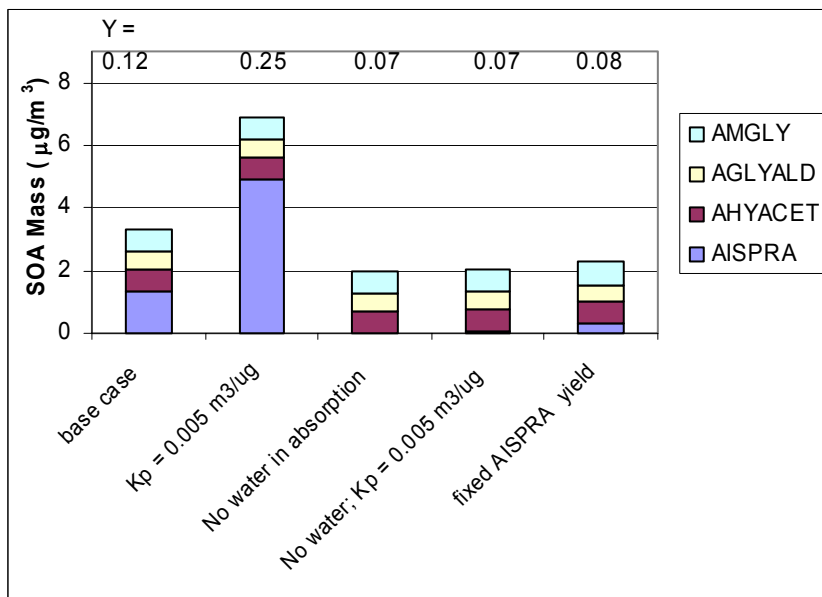


Figure 4. Mass and yield of isoprene SOA under different scenarios that affect the partition of ISPRAER.

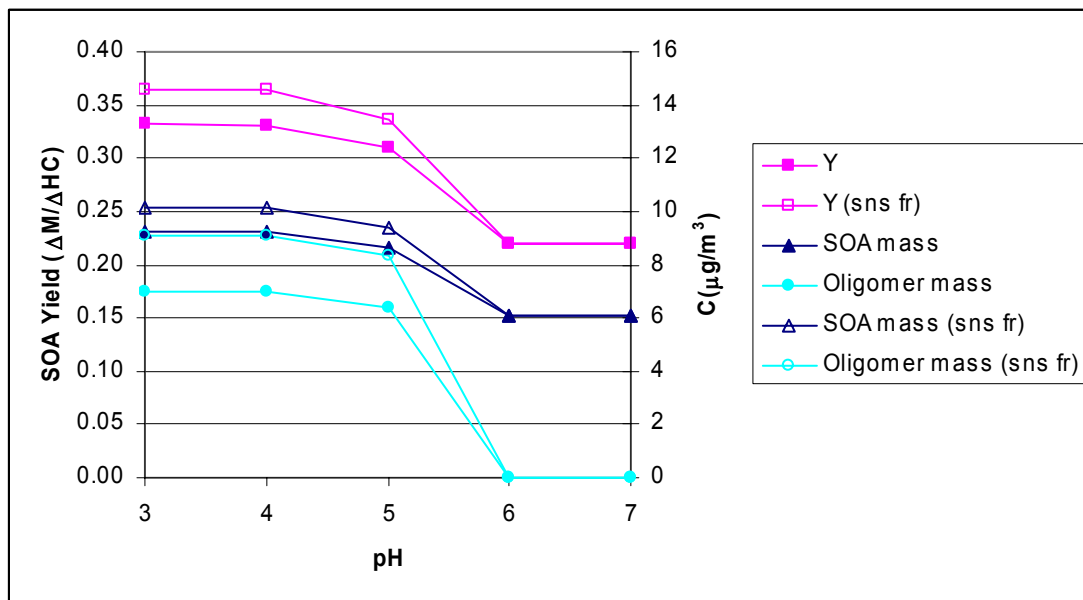


Figure 5. Yield and concentrations of total SOA and oligomers under the base case (solid symbols) and in the sensitivity case where all APINAER2 products are assumed to undergo oligomerization (sns fr denotes cases where the fraction of condensable products = 1; open symbols).

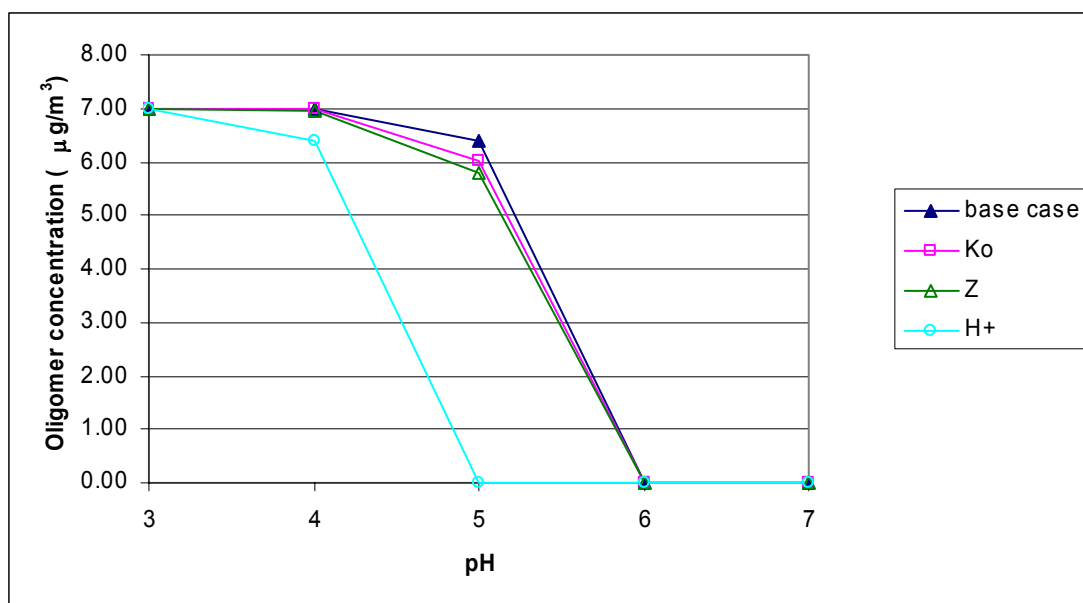


Figure 6. Concentrations of oligomers as a function of pH in sensitivity cases where parameters in the calculation of the effective partition constant due to oligomerization is changed. (K_o denotes the case where $K_{o,eff}$ is reduced; Z denotes the case where z is reduced and H^+ denotes the case where the pH value required to activate oligomerization is reduced.)